Declining, seasonal-varying emissions of sulfur hexafluoride from the United States

Lei Hu[1*], Deborah Ottinger[2], Stephanie Bogle[2], Stephen A. Montzka[1], Philip L. DeCola[3,4], Ed Dlugokencky[1], Arlyn Andrews[1], Kirk Thoning[1], Colm Sweeney[1], Geoff Dutton[1,5], Lauren Aepli[2], Andrew Crotwell[1,5]

[1] Global Monitoring Laboratory, US National Oceanic and Atmospheric Administration, Boulder, CO, USA
[2] Climate Change Division, US Environmental Protection Agency, Washington D.C., USA
[3] Department of Atmospheric and Oceanic Sciences, University of Maryland, College Park, MD, USA
[4] GIST.Earth LLC, Washington DC, USA
[5] Cooperative Institute for Research in Environmental Sciences, University of Colorado-Boulder, Boulder, CO, USA

*Correspondence to lei.hu@noaa.gov

Abstract

Sulfur hexafluoride (SF_6) is the most potent greenhouse gas and its atmospheric abundance, albeit small, has been increasing rapidly. Although SF_6 is used to assess atmospheric transport modeling and its emissions influence the climate for millennia, SF_6 emission magnitudes and distributions have substantial uncertainties. In this study, we used NOAA's ground-based and airborne measurements of SF_6 to estimate SF_6 emissions from the U.S. between 2007 and 2018. Our results suggest a substantial decline of U.S. SF_6 emissions, a trend also reported in the U.S. Environmental Protection Agency (EPA)'s national inventory submitted under the United Nations Framework on Climate Change, implying that U.S. mitigation efforts have had some success. However, the magnitudes of annual emissions derived from atmospheric observations are 40 – 250% higher than the EPA national inventory and substantially lower than the Emissions Database for Global Atmospheric Research inventory. The regional discrepancies between atmosphere-based estimate and EPA's inventory suggest that emissions from electric power transmission and distribution (ETD) facilities and an SF_6 production plant that did not or does not report to EPA may be underestimated in the national inventory. Furthermore, the atmosphere-based estimates show higher winter than summer emissions of SF_6. These enhanced wintertime emissions may result from increased maintenance of ETD equipment in southern states and increased leakage through aging brittle seals in ETD in northern states in winter. The results of this study demonstrate the success of past U.S. SF_6 emission mitigations, and suggest substantial additional emission reductions might be achieved through efforts to minimize emissions during servicing or through improving sealing materials in ETD.

Short Summary

Effective mitigation of greenhouse gas (GHG) emissions relies on an accurate understanding of emissions. Here we demonstrate the added value of using inventory- and atmosphere-based approaches for estimating U.S. emissions of SF_6, the most potent GHG known. The

results suggest a large decline in U.S. SF_6 emissions, shed light on the possible processes causing the differences between the independent estimates, and identify opportunities for substantial additional emission reductions.

Introduction

Sulfur hexafluoride (SF_6) is the greenhouse gas (GHG) with the largest known 100-year global warming potential (GWP) (i.e., 25,200) and an atmospheric lifetime of 580 - 3200 years (Forster et al., 2021; Ray et al., 2017). SF_6 is primarily used in electrical circuit breakers and high-voltage gas-insulated switchgear in electric power transmission and distribution (ETD) equipment, and its emissions occur during manufacturing, use, servicing, and disposal of the equipment. There is also usage and associated emissions of SF_6 from production of magnesium and electronics. Because of its extremely large GWP and long atmospheric lifetime, emissions of SF_6 accumulate in the atmosphere and will influence Earth's climate for thousands of years. Since 1978, global emissions of SF_6 have increased by a factor of 4 due to rapid expansion of the ETD systems and the metal and electronics industries (Rigby et al., 2010; Simmonds et al., 2020). As a result, the global atmospheric mole fractions and radiative forcing of SF_6 have increased by 14 times over the same period. In 2019, the radiative forcing of SF_6 was 6 mW m^{-2} or 0.2% of total radiative forcing from all long-lived GHGs, making it the 11th largest contributor to the total radiative forcing among all the long-lived greenhouse gases and the 7th largest contributor among gases whose atmospheric concentrations are still growing (i.e., other than CFCs and carbon tetrachloride) (Gulev et al., 2021). If global SF_6 emissions continue at the 2018 rate (9 Gg yr^{-1}) into the future, the global atmospheric mole fraction and radiative forcing of SF_6 will linearly increase by another factor of 4 by the end of the 21st century (Fig. S1). If global emissions of SF_6 continue to rise at the same rate as 2000 – 2018, the global atmospheric mole fraction and radiative forcing of SF_6 will increase by another factor of 10 by the end of the 21st century (Fig. S1). Consistent with the large GWP of SF_6 emissions and its importance for influencing climate for many years, national emissions of this gas are reported under the United Nations Framework Convention on Climate Change (UNFCCC) annually by the U.S. Furthermore, accurate estimates of the magnitude and distribution of SF_6 emissions are also important in studies to refine our understanding of atmospheric transport processes in the troposphere and stratosphere (Orbe et al., 2021; Waugh et al., 2013; Denning et al., 1999; Gloor et al., 2007; Peters et al., 2004; Schuh et al., 2019; Ray et al., 2017; Maiss and Levin, 1994; Harnisch et al., 1996).

Although global emissions of SF_6 can be well constrained with knowledge of its observed remote-atmosphere growth rates and its atmospheric lifetime, large uncertainties remain in the magnitude and distribution of SF_6 emissions on national and regional scales. For example, the total annual national emissions reported to the UNFCCC summed from its Annex I (mostly developed countries) and some non-Annex I (mostly developing) countries (including China, one of the large SF_6 emitting countries) account for only 50% of global annual SF_6 emissions derived from atmospheric observations for the analyzed years (1990 – 2007) (Simmonds et al., 2020; Rigby et al., 2010; Levin et al., 2010). This difference between activity-based inventory ("bottom-up") estimates and atmosphere-based ("top-down") estimates may result from underestimates of emissions by activity-based inventories (Simmonds et al., 2020; Rigby et al., 2010; Levin et al., 2010; Weiss and Prinn, 2011) as well as from substantial emissions from non-reporting countries. The results of activity-based inventories are sensitive to estimated activity levels and, especially, emission rates. In the Emission Database for Global Atmospheric Research (Janssens-Maenhout,

2011; Crippa et al., 2020), U.S. SF_6 emissions were up to five times larger than the emissions estimated by the U.S. Environmental Protection Agency (EPA) and in their reporting to the UNFCCC (U.S. Environmental Protection Agency, 2022a) (Fig. 1). The causes for this large difference are not fully known, but appear to arise largely from the ETD sector (Fig. S2). Uncertainties in EPA's emissions estimates were also illuminated by a comparison between the SF_6 usage inferred from the user reports (which form the basis of EPA's emissions estimates) and the SF_6 usage inferred from suppliers' reports, which showed that supplier-based estimates were 70% higher than user-based estimates in 2012 (Ottinger et al., 2015).

Against this backdrop, we estimated U.S. SF_6 emissions between 2007 and 2018 using inverse modeling of atmospheric mole fraction measurements made from ground-based and airborne whole-air flask samples collected from the U.S. National Oceanic and Atmospheric Administration (NOAA) Global Greenhouse Gas Reference Network (Fig. 1). The analysis provides robust emission estimates by region and season for the contiguous U.S. (CONUS). Our study offers an independent estimate that complements the current U.S. inventory-based national emission reporting of SF_6 to the UNFCCC. This effort exemplifies the quality assurance guidance laid out in the *2019 Refinement to the 2006 IPCC Guidelines for National Greenhouse Gas Inventories*, which states "Atmospheric measurements are being used to provide useful quality assurance of the national greenhouse gas emission estimates. Under the right measurement and modelling conditions, they can provide a perspective on the trends and magnitude of greenhouse gas (GHG) emission estimates that is largely independent of inventories" (Maksyutov et al., 2019). In fact, the United Kingdom, Switzerland, and Australia have already included top-down atmosphere-based emission estimates in the QA/QC section of their national GHG emission reporting to UNFCCC (Fraser et al., 2014; Henne et al., 2016; Manning et al., 2021). The United States also started to include top-down estimates of four major hydrofluorocarbons (HFCs) as a comparison to the U.S. national GHG inventory reporting in 2022 (U.S. Environmental Protection Agency, 2022a). Derived national and regional SF_6 emissions from this analysis are accessible through NOAA's U.S. Emission Tracker for Potent GHGs website (https://gml.noaa.gov/hats/US_emissiontracker).

Methods

Top-down atmosphere-based SF_6 emission estimates were derived using inverse modeling of NOAA's long-term atmospheric measurements of SF_6 (https://gml.noaa.gov/aftp/data/hats/sf6/Data_in_Hu_et_al_2023/). Measurements made over North America were based on air samples collected by discrete flasks from tall towers and aircraft. The tall tower flask samples were typically collected every one to two days and airborne flask-sample profiles were collected once or twice per month between 0 and 8 km above sea level. Measurements made outside North America were from weekly whole-air samples collected globally, generally at remote locations far away from emission sources (https://gml.noaa.gov/dv/site/). All the whole-air flask samples were shipped to Boulder and analyzed by a Gas Chromatography with Electron Capture Detector (GC-ECD) for SF_6. Uncertainty of each SF_6 flask measurement is approximately 0.04 to 0.05 ppt, which includes uncertainties related to short-term measurement noise, long-term measurement reproducibility, and calibration scale transfer from gravimetric standards to working standards.

Mole fraction enhancements of SF_6 over the contiguous U.S. (Fig. 1) relative to SF_6 mole fractions in air measured upwind were then estimated for deriving U.S. emissions. These enhancements were estimated by referencing them to "background" mole fractions that were derived using three different approaches. These approaches are similar to previous inversion analyses for other atmospheric trace gases (Hu et al., 2021; Hu et al., 2017). In all three approaches, we constructed an empirical 4-dimensional mole fraction field based on measurements made in air over the Pacific and Atlantic Ocean basins and in the free troposphere above 3 km over North America, so that it contains vertical and horizontal gradients of mole fractions measured in the remote atmosphere over time. From this empirical background, we then extracted the mole fraction at the sampling time and location of each observation and used it as our first background estimate. In the second approach, we considered 500 air back-trajectories associated with each observation. Five hundred background estimates were extracted from this empirical background at the locations where the air back-trajectories exited the North American domain horizontally or where they were aloft above 5 km. In most cases, the majority of particles exited North America horizontally or vertically within 10 days, but for those that remained within the domain after 10 days, background values were derived from their positions 10 days after sampling. For midcontinent and eastern sites, there were up to 20% of particles remained within the domain after 10 days. The 500 background estimates were averaged to obtain the background mole fraction estimation for that observation. In the third approach, we assessed potential biases in the background estimate from the second approach, particularly because there was a small fraction of back-trajectories ending up in the planetary boundary layer in North America after 10 days. Background mole fractions for these particles were likely higher than estimated using the marine boundary layer information. To minimize such biases, we corrected our background estimates from the second approach based on their differences with measurements made within North America that had small surface sensitivities over populated areas (Hu et al., 2017).

SF_6 mole fraction enhancements estimated in observations at North American sites were then incorporated into a regional inverse model to estimate U.S. national and regional emissions, following the same methodology as described in our previous inversion studies for other anthropogenic gases (Hu et al., 2017; Hu et al., 2015; Hu et al., 2016). In regional inversions, we assume a linear relationship between atmospheric mole fraction enhancements and upwind emissions. The linear operator is called a 'footprint' or the Jacobian matrix, representing the spatial and temporal sensitivity of atmospheric mole fraction observations to emissions. Footprints were computed by two transport models, the coupled Weather Research and Forecasting - Stochastic Time-Inverted Lagrangian Transport model (WRF-STILT) (Nehrkorn et al., 2010) and the Hybrid Single-Particle Lagrangian Integrated Trajectory model (Stein et al., 2015) driven by the North American Mesoscale Forecast System (HYSPLIT - NAMs). The WRF field has 41 pressure levels and a horizontal resolution of 10-km in North America and 40-km outside of North America. The NAMs meteorology has a 12-km resolution and 40 sigma-pressure levels. Before March 2009, when NAMs was not available; we used NAM-12 meteorology, which only has 26 vertical levels. NAMs or NAM-12 was nested with the U.S. National Centers for Environmental Prediction (NCEP) 0.5^o Global Data Assimilation System (GDAS0.5) with 55 sigma-pressure levels. Both WRF-STILT and HYSPLIT-NAMs were run with 500 particles back in time for 10 days (e.g., Miller et al., 2013; Nevison et al., 2018; Miller et al., 2012; Gerbig et al., 2003). In each run, particles were released at the sampling inlet heights. Footprints were then calculated by

integrating particles between the modeled surface to modeled boundary layer in each grid at each timestep (Lin et al., 2003).

A Bayesian inverse modeling technique (Rodgers, 2000) was implemented, where a prior emission field or "a priori" was required. The model adjusts magnitudes and distributions of the a priori at a $1^o \times 1^o \times$ weekly resolution, such that the posterior solution of emissions better represents the observed magnitudes, and horizontal and vertical gradients of mole fraction enhancements observed in the U.S. Here, we used two different temporally-constant prior emission fields. The first one was from the Emissions Database for Global Atmospheric Research version 4.2 (EDGARv4.2) with a U.S. total SF_6 emission of 1.8 Gg yr^{-1} in 2008, We used the 2008 EDGARv4.2 estimate and applied it for all years between 2007 – 2018 in our inversions. EDGARv4.2 was the most recent grid-scale product offered by EDGAR at the time we conducted our inversions. EDGAR version 7.0 (EDGARv7.0) became available only after this work was submitted in late September of 2022. It extends this inventory emission through 2021 and its U.S. total and regional SF_6 emissions for earlier years are similar to those in EDGARv4.2 (Figs. 1 and 2). Given the similarities of EDGAR v7.0 with v4.2 in distribution and magnitude and the insensitive nature of our posterior results to these aspects of the prior (see below), we did not rerun inversions with EDGARv7.0 as a priori. The second a priori includes a U.S. total emission of 0.4 Gg yr^{-1} for 2007 – 2018. It was distributed by population density from the Gridded Population of the World (GPW) v4 dataset (https://sedac.ciesin.columbia.edu/data/collection/gpw-v4, last access: 15 March 2019). The weight between the prescribed prior emissions and atmospheric observations in the final posterior emission solution was determined by the values in the prior emission error covariance matrix and the model-observation mismatch covariance matrix, which were calculated from the maximum likelihood estimation (Michalak et al., 2005; Hu et al., 2015).

In each inversion, the derived $1^o \times 1^o \times$ weekly emissions and emission uncertainties were aggregated to derive emissions and uncertainties at regional and national scales and at monthly and annual time steps. When calculating the posterior uncertainty, we considered the temporal and spatial correlations of posterior errors in the derived full posterior emission covariance matrix. The final reported emissions and emission uncertainties include results from a total of 12 inversions that have two representations of transport, two prior emission fields, and three background estimates. Assume μ_i and σ_i represent the posterior emission estimate and its associated 1-sigma error for the *i* th inversion. Our final estimate of emissions and its associated uncertainty discussed in the text were calculated as the mean posterior emission and the 2-sigma uncertainty ($2\sigma_t$) derived from Eq. (1).

$$\sigma_t = \sqrt{\frac{{\sigma_1}^2+{\sigma_2}^2+\cdots+{\sigma_{12}}^2}{12} + {\sigma_s}^2} \quad (1)$$

where σ_s denotes 1-sigma spread or variability of the posterior emissions derived from all 12 inversions.

Results and discussion

Declining SF_6 emissions from the U.S.

The U.S. recognized that it had significant emissions of SF_6 in the 1990s and has taken steps to reduce its national emissions. In the U.S., 60 – 80% of SF_6 emissions have historically been from the ETD sector (U.S. Environmental Protection Agency, 2022a) (Fig. 1). Outside the ETD sector,

smaller amounts of SF_6 are used in semiconductor manufacturing processes as a source of fluorine to etch patterns onto chips and to clean thin film deposition chambers, and SF_6 is also used as a cover gas in magnesium production and casting processes to prevent rapid oxidation of molten magnesium. Both of these uses result in emissions. SF_6 emissions from magnesium processes accounted for roughly 15 – 30 % of the U.S. total emissions reported by EPA between 1990 and 2018 (Fig. 1). While the magnitude of SF_6 emissions from the electronics manufacturing sector has not changed much over time, its share of total U.S. SF_6 emissions in the EPA inventory has increased from 2% in 1990 to 14% in 2018 as emissions from other industries have decreased.

Since 1999, the U.S. EPA has worked with the electric power industry through the voluntary SF_6 Emission Reduction Partnership for Electric Power Systems to identify, recommend, and implement cost-effective solutions to reduce SF_6 emissions. There have also been regulations at the state level to reduce SF_6 emissions from the ETD sector (U.S. Environmental Protection Agency, 2022a). In addition, the EPA operated voluntary partnership programs with the semiconductor and magnesium industries from the late 1990s through 2010 to understand and reduce their emissions. These national- and state- level mitigation strategies, along with an increase in the market price of SF_6 during the 1990s, have resulted in a substantial reduction in total U.S. SF_6 emissions since 1990 (Fig. 1). In addition, before 2011, SF_6 was likely emitted from an SF_6 production plant that ceased producing SF_6 in 2010, according to data reported to the U.S. EPA. Total U.S. SF_6 emissions estimated by the EDGAR version 4.2 or 7.0 inventory showed an absolute decline over this period similar to that in the EPA National Greenhouse Gas Inventory (GHGI), but EDGAR emissions were substantially larger on average (Fig. 1). Note that although the U.S. national total in EDGARv7.0 suggests lower emissions than EDGARv4.2, this difference arises only in the magnesium production sector. There were slightly higher emissions from the ETD and electronics industries in EDGARv7.0 than in EDGARv4.2 over the U.S. (Fig. S2).

Consistent with the inventory reports, the independent, atmospheric observation-based results presented here suggest a large decline of U.S. total SF_6 emissions, confirming the success of U.S. SF_6 emission mitigation efforts. The atmospheric observation-based emissions declined from 0.93 ($\pm 0.19, 2\sigma$) Gg yr^{-1} in 2007 – 2008 to 0.37 ($\pm 0.10, 2\sigma$) Gg yr^{-1} in 2017 – 2018 (Table 1 and Fig. 1). The 0.56 ± 0.21 (2σ) Gg yr^{-1} drop in SF_6 emissions from 2007 – 2008 to 2017 – 2018 is equivalent to a reduction of 13 ± 7 million tons of CO_2 emission, when using the 100-year global warming potential that was used in the EPA GHGI (GWP_{100} = 22800).

Although both the atmosphere-based top-down and inventory-based bottom-up estimates show declining trends for total U.S. SF_6 emissions, the estimated emission magnitudes are quite different. In 2007 – 2008, the atmosphere-based emissions fall between the EDGARv7.0 and EPA's GHGI estimates; but the difference between the atmosphere-based estimate and EDGARv7.0 increases over time, whereas the difference between the atmosphere-derived estimate and EPA's inventory decreases over time. After 2011, the atmosphere-based emission estimates are 0.93 ($\pm 0.07, 2\sigma$) Gg yr^{-1} (a factor of 3.4) lower than EDGARv7.0 and only about 0.15 ($\pm 0.07, 2\sigma$) Gg yr^{-1} (35%) higher than the EPA's GHGI (U.S. Environmental Protection Agency, 2022a). The improved agreement between the EPA GHGI and the atmosphere-based estimates may be associated with more accurate emission information used to inform the EPA's GHGI after 2010. Before 2011, the SF_6 emission estimate in the EPA GHGI was primarily informed by reporting through the voluntary Partnership Programs between EPA and various industries (Rand, 2012) described above.

In 2011, EPA established its greenhouse gas reporting program (GHGRP), requiring facility-based reporting of greenhouse gas (GHG) data and other relevant information from large GHG emission sources ($\geq$ 25,000 CO_2-equivalent metric tons of GHG emissions per year). Although smaller emitters are not required to report their emissions, this program provides more complete emission information than had been available prior to 2011. For example, from 1999 to 2010, ETD facilities representing an estimated 60% of the emitting activity reported their SF_6 emissions to EPA through EPA's voluntary reporting program. After 2010, ETD facilities representing an estimated 70% of the emitting activity began reporting their emissions to EPA under the GHGRP.

A variety of factors may be contributing to the difference observed between the SF_6 emissions estimates from atmospheric measurements and the estimates developed for the U.S. EPA GHGI. The largest potential contributor to the difference is a possible underestimate by the GHGI of emissions from ETD facilities that do not report to EPA, or that did not report to EPA until they were required to report by the GHGRP starting in 2011. Emissions from non-reporting facilities are currently estimated based on the uncertain assumption that the emission rate per mile of transmission line (transmission mile) for non-reporting facilities has been the same, on average, as that for reporting facilities in each year of the time series. However, the emission rate per transmission mile has varied significantly across facilities and over time due to a variety of factors, including the age of the electrical equipment, maintenance practices, local regulations, and the quantity of SF_6-containing equipment per transmission mile (SF_6 nameplate capacity). Among reporting facilities, the emission rate has fallen from an average of 0.7 kg per transmission mile in 1999 to 0.2 kg per transmission mile in recent years, with emission rates declining most quickly in the first three years of reporting (i.e., 1999-2001 for Partners, 2011-2013 for facilities that began reporting under the GHGRP). This implies that reporting itself may drive emission reductions. Thus, it is plausible that the emission rate of non-reporting facilities has fallen more slowly than that of reporting facilities.

In the years prior to 2011, there are several additional factors that may be contributing to the underestimate of SF_6 emissions by the GHGI, compared to the atmosphere-based estimates. One potentially significant factor is that the GHGI does not currently account for SF_6 emissions from the SF_6 production plant that operated in Metropolis, Illinois, up until 2010. This plant never reported its emissions to EPA; but based on production capacity data for the plant from 2006 and the broad range of emission factors observed for production of SF_6 and other fluorinated gases, the plant's SF_6 emissions would likely have ranged between 0.03 and 0.3 Gg yr^{-1}. Notably, the region showing the largest drop in the atmosphere-derived emissions between 2008 and 2011-2018 includes Metropolis, Illinois (Fig. S3). Although emissions from this plant have not been included in previous GHGIs, the discrepancy highlighted here points to potential significant contributions from this plant before 2011 (and other fluorinated gas production facilities) that will be included in future submissions of the GHGI.

Other factors that may account for a small portion of the post-2011 difference is an underestimate of emissions of SF_6 from electronics manufacturing by a factor of 2 (equivalent to ~ 0.02 Gg yr^{-1}). In the GHGI, the EPA adjusted the time series of GHGRP-reported data for 2011 through 2013 to ensure time-series consistency using a series of calculations that took into account the characteristics of a facility (e.g., wafer size and abatement use) and updated default emission factors and destruction and removal efficiencies. These updates reflected improved activity data

and not changes to emission rates, and resulted in an increase in SF_6 emissions estimates by 95% from electronics manufacturing. Finally, a similar improvement for time series consistency is planned for pre-2011 estimates and is expected to result in a similar relative increase in estimated SF_6 emissions from the electronics sector for those years.

U.S. regional SF_6 emissions

We also investigated regional emissions derived from atmospheric inversions and from EPA's recently created Inventory of U.S. Greenhouse Gas Emission and Sinks by State (U.S. Environmental Protection Agency, 2022b) to understand the distribution of SF_6 emissions and how various regions contribute to the difference between the atmosphere- and inventory- derived U.S. total emissions. Note that the EPA GHGI was only able to allocate 20 – 30 % of ETD emissions to a single state by facility location (i.e. when the facility was only in one state). The remaining emission was distributed based on a national average emission factor (kg of SF_6 per transmission mile). Because of this limited regional resolution, we expect some limitations in the regional estimates of the GHGI. However, this comparison with atmosphere-based estimates helps assess the robustness of the regional estimates.

The atmosphere-based emission estimates suggest that about 80% of the U.S. total SF_6 emissions were contributed by three regions: the northeast, central north, and central south (Table 1; Figs. 2). Regional SF_6 emissions corresponding to the GHGI calculated using the EPA's Inventory of U.S. Greenhouse Gas Emission and Sinks by State (U.S. Environmental Protection Agency, 2022b) were distributed slightly differently. For the southeast, west, and mountain regions, EPA's regional emissions agree well with emissions estimated from atmospheric observations, but they are lower than the atmosphere-derived emissions in the northeast for the entire study period and in the central north and central south during 2007 – 2010. Such regional differences were expected due to the limited regional resolution of the GHGI for emissions from ETD. For regions that predominantly had emissions from the ETD sector, the difference is likely more dependent on how similar the ETD emissions in the region are to the national average. This method could result in an underestimate of emissions in the regions like the northeast where the average emission rate is expected to be higher than the national average based on historical data submitted to the EPA by facilities in the region. Higher regional emission rates in the northeast could be due in part to the region containing more gas-insulated equipment per transmission mile and the presence of older transmission systems (i.e. older, leakier equipment). The national average emission factor may be more appropriate for the mountain, central north, and central south regions. This is because regional emission factors that are based only on GHGRP reported emissions from facilities that reside entirely within the region, are similar to a national average in these regions. Better agreement in the western region may be also associated with the incorporation of the California Air Resource Board estimate for SF_6 from California in the GHGI.

For the central north and central south regions, the atmosphere-derived emissions were higher in 2007 – 2010 and show a larger declining trend than the EPA GHGI. The larger discrepancy in the central north and central south before 2011 may be due in part to the unaccounted emissions by GHGI from the SF_6 production facility in Metropolis, Illinois, described above, which ceased producing SF_6 in 2010. This facility is located right at the border between the central north and central south regions, so it is likely that emissions from it could have been attributed to one or both adjacent regions in the atmospheric inversions.

Besides the EPA GHGI, we also compared our top-down estimate with the EDGAR inventories (EDGARv4.2 and EDGARv7.0). Results suggest that emissions estimated by the EDGAR are higher than the atmosphere-derived emissions and the EPA's inventory estimates for all regions across the U.S., especially in the western and northeast regions (Fig. 2).

Significant seasonality detected in U.S. SF_6 emissions

The monthly SF_6 emissions derived from our inverse analysis of atmospheric concentration measurements reveal a prominent seasonal cycle with higher emissions in winter for all 12 years of this analysis (Fig. 3a). On average, the magnitude of winter SF_6 emissions is about a factor of 2 larger than summer emissions summed across the contiguous U.S. (Fig. 3a). This seasonality is most likely from the use, servicing, and disposal of ETD equipment, as SF_6 emissions from magnesium production, electronics production, and manufacturing of ETD equipment are expected to be aseasonal. Consistent with this hypothesis, winter-to-summer ratios of total U.S. SF_6 emissions derived for individual years significantly correlate at a 99% confidence level ($r = 0.71$; $P = 0.01$) with the annual fractions of national emissions contributed by the ETD sector reported by EPA (Fig. 3c). Moreover, this robust relationship also holds regionally ($r = 0.84$; $P = 0.02$) (Fig. 3c). The largest seasonal variation in emissions is detected in the southeast and central south regions of the U.S., where the ETD sector accounted for more than 85% of the regional total emissions (Figs. 2, 3b, and 3c). In these southern regions, the winter emissions were higher than summer emissions by more than a factor of 2, whereas in the central north, where the ETD sector accounted for about 50% of the regional total emissions, the mean winter-to-summer emission ratio was less than 1.5 (Figs. 2 and 3c).

The enhanced winter emissions in the southern states are consistent with the fact that more servicing is performed on electrical equipment and transmission lines over this region in the cooler months (information provided by Mr. B. Lao at the DILO Company, Inc.), when electricity usage is lower compared to other seasons (U.S. Energy Information Administration, 2020). This suggests that the enhanced seasonal SF_6 emission may be associated with the season during which electrical equipment repair and servicing is enhanced. In the northern states, the higher winter than summer emissions may relate to increased leakage through more brittle seals in the aging electrical transmission equipment due to increased thermal contraction in winter (Du et al., 2020). This winter-to-summer ratio in the northeast is somewhat higher than in the other northern regions (Fig. 3b), which may reflect the fact that the electrical power grid is denser (U.S. Federal Emergency Management Agency, 2008) and ETD is the primary emitting source of SF_6 over the northeast region.

Given that the ETD sector may be the primary cause for seasonally-varying emissions in the U.S., we next assessed changes in seasonality over time and their implication for changes in sector-based emissions from 2007 to 2018. The most notable feature of the time series (Fig. S4) is that the largest seasonal cycle occurred in 2009 when the economic recession took place. The 2009 recession resulted in a significant drop in the production of magnesium and electronics (U.S. Environmental Protection Agency, 2021), but little (if any) change to the ETD infrastructure and associated servicing practices is likely to have occurred. Thus, ETD emissions represent a larger fraction of the total U.S. SF_6 emissions in that year. In addition, the winter-to-summer emission ratios appear smaller before the 2009 peak (i.e., in 2007 – 2008) than after it (in 2011 – 2018).

This may imply that emissions from the ETD sector accounted for a growing fraction of total emissions through this entire period.

Conclusions and implications

SF_6 is a potent industrially-produced greenhouse gas with an extremely long atmospheric lifetime. It is a trace gas that is primarily used in the electrification of the energy sector. In the past five decades, global emissions, concentrations, and radiative forcing of SF_6 have substantially increased due to growing energy demand. Without effective emission mitigation efforts worldwide, the climate impact of SF_6 will continue to rise in the future. In contrast to the global emission trend, U.S. SF_6 emissions have decreased substantially since the 1990s. These decreases are documented in EPA's emission inventories reported annually to the UNFCCC and in the new results reported here from an inverse analysis of atmosphere concentration measurements. These independently-derived U.S. emission records demonstrate substantial success by U.S. industry in coordination with the EPA in mitigating SF_6 emissions.

The magnitude of SF_6 emissions derived from atmospheric inversions are higher than those reported in the EPA GHGI but lower than EDGAR; but the difference between the EPA GHGI and atmosphere-derived estimates become substantially smaller after 2011, when national GHG reporting became mandatory, implying that that the shift from voluntary to mandatory emission reporting by industry increased the accuracy of the inventory. However, differences remain between the emissions estimated from these independent methods, which may relate to the uncertain assumptions about ETD-related emission rates per mile from non-reporting facilities in the GHGI. Although the EPA GHGI may underestimate SF_6 emissions, its contribution to the global "missing" source of SF_6 is small. More specifically, the total SF_6 emissions summed from all reporting countries to the UNFCCC are only half of the global emissions derived from global-scale observed concentration trends; in other words, there are ~ 4 Gg SF_6 yr^{-1} or 100 million tons of CO_2-equivalent per year of SF_6 emissions still "missing" in the global GHG accounting system. The underestimate of the U.S. GHGI only contributed 14% in 2007 – 2008 and only 3% after 2011 to this global SF_6 emission gap, implying either large underreporting of SF_6 emissions from other reporting countries or large emissions from non-reporting countries.

Regional emissions from atmospheric inversions were compared with the recently available disaggregation of the EPA GHGI by state to provide an initial assessment on the emission distribution of SF_6 estimated from the GHGI. Good agreement was noted in some regions but not others. Combining the spatial discrepancies with processes used for constructing the GHGI, we were able to identify regions where applying a national average emission factor may be inappropriate and where historical emissions of a facility (the SF_6 production plant in Metropolis, Illinois) are currently not accounted for but may have been significant.

Finally, the atmosphere-derived results further suggest a strong seasonal cycle in U.S. SF_6 emissions from electric power transmission and distribution for the first time, with wintertime emissions twice as large as summertime emissions. This seasonal cycle is thought to be strongest in southern states, where servicing of ETD equipment is typically performed in winter. The seasonal cycle is likely enhanced additionally by increased leakage from ETD equipment during the winter, when cold weather makes sealing materials more brittle and therefore less effective.

This newly discovered seasonal emission variation implies that further larger reductions of SF_6 emission in the U.S. might be achievable through efforts to minimize losses during equipment maintenance and repairs, and through the use of improved sealing materials in ETD equipment.

The 2019 Refinements to the 2006 IPCC Guidelines for National Greenhouse Gas Inventories suggest that atmospheric inversion-derived emissions be considered in the quality assurance, quality control and verification of the national GHG inventory reporting. It is anticipated that the consideration of an independent estimate will lead to more accurate inventories. The work presented here, however, suggests that a collaboration between these communities can provide much more. In the case of SF_6, the result has been not only an improved understanding of emission magnitudes, but also a better grasp of the processes that lead to emissions and the identification of substantial new emission mitigation opportunities, thereby pointing the way towards a more effective and efficient means to minimize and reduce national greenhouse gas emissions.

Data availability

Atmospheric SF_6 observations used in this analysis are available at https://gml.noaa.gov/ccgg/obspack/data.php. Data included in our inversion can be downloaded at https://gml.noaa.gov/aftp/data/hats/sf6/Data_in_Hu_et_al_2023/. The marine boundary layer reference for SF_6 can be downloaded from https://gml.noaa.gov/ccgg/mbl/data.php. Atmospheric observation-derived U.S. national and regional emissions from this analysis are accessible through the US Emission Tracker for Potent GHGs (https://gml.noaa.gov/hats/US_emissiontracker). SF_6 emissions reported to the GHGR are available at https://www.epa.gov/enviro/greenhouse-gas-customized-search.

Author contributions

LH developed the inversion framework, performed the analysis, and wrote the paper with DO, SB, and SM. Significant edits and inputs were also from PD and ED. DO and SB made and provided EPA SF_6 emission estimates. PD, SM, and LH initiated this project. LH, DO, SB, SM, and PD worked on the interpretation of the results. ED led the NOAA SF_6 measurements. PD coordinated the discussion between NOAA and EPA colleagues. AA led the NOAA tower sampling network, provided the 4D empirical background estimates of SF_6 and WRF-STILT footprints. KT and GD helped with improving the inversion code. KT and LH computed the HYSPLIT footprints. CS led the NOAA aircraft sampling network. LA contributed the construction of EPA SF_6 emission estimates. AC contributed to NOAA SF_6 measurements.

The views expressed in this article are those of the authors and do not necessarily represent the views or policies of the U.S. Environmental Protection Agency.

Acknowledgement

This work was funded in part by the Grantham Foundation, NOAA Climate Program Office's Atmospheric Chemistry, Carbon Cycle, and Climate (AC4) and Climate Observations and Monitoring (COM) programs (NA21OAR4310233), and the NOAA Cooperative Agreement with CIRES, NA17OAR4320101. We thank Mr. Billy Lao at the

DILO company, Inc. for insights on the timing of repairing and servicing of electrical equipment. We thank Dr. Bradley Hall for maintaining the primary SF_6 calibration scale for all NOAA SF_6 measurements. We thank Jon Kofler, Kathryn McKain, Don Neff, Sonja Wolter, Jack Higgs, Molly Crotwell, Patrick Lang, Eric Moglia, and Monica Madronich for facilitating flask sampling and measurements. We thank Dr. Andy Jacobson for providing SF_6 simulations from the SF_6 Model Inter-comparison Project even though they were not included in the final publication of this analysis.

References

Crippa, M., Solazzo, E., Huang, G., Guizzardi, D., Koffi, E., Muntean, M., Schieberle, C., Friedrich, R., and Janssens-Maenhout, G.: High resolution temporal profiles in the Emissions Database for Global Atmospheric Research, Scientific Data, 7, 121, 10.1038/s41597-020-0462-2, 2020.

Denning, A. S., Holzer, M., Gurney, K. R., Heimann, M., Law, R. M., Rayner, P. J., Fung, I. Y., Fan, S.-M., Taguchi, S., Friedlingstein, P., Balkanski, Y., Taylor, J., Maiss, M., and Levin, I.: Three-dimensional transport and concentration of SF_6 A model intercomparison study (TransCom 2), Tellus B: Chemical and Physical Meteorology, 51, 266-297, 10.3402/tellusb.v51i2.16286, 1999.

Du, B., Zhang, Z., Qiao, Y., Suo, S., Luo, H., and Li, X.: Online sealing of SF_6 leak for Gas insulated switchgear, IOP Conference Series: Earth and Environmental Science, 514, 042021, 10.1088/1755-1315/514/4/042021, 2020.

Forster, P., Storelvmo, T., Armour, K., Collins, W., Dufresne, J. L., Frame, D., Lunt, D. J., Mauritsen, T., Palmer, M. D., Watanabe, M., Wild, M., and Zhang, H.: The Earth's Energy Budget, Climate Feedbacks, and Climate Sensitivity, in: Climate Change 2021: The Physical Science Basis. Contribution of Working Group I to the Sixth Assessment Report of the Intergovernmental Panel on Climate Change, edited by: Masson-Delmotte, V., Zhai, P., Pirani, A., Connors, S. L., Pean, C., Berger, S., Caud, N., Chen, Y., Goldfarb, L., Gomis, M. I., Huang, M., Leitzell, K., Lonnoy, E., Matthews, J. B. R., Maycock, T. K., Waterfield, T., Yelekci, O., Yu, R., and Zhou, B., Cambridge University Press, 2021.

Fraser, P., Dunse, B., Krummel, P. B., Steele, P., and Derek, P.: Australian HFC, PFC, Sulfur Hexafluoride and Sulfuryl Fluoride emissions, Report prepared for Australian Goverment Department of the Environment, by the centre for Australian Weather and Climate Research, CSIRO Oceans and Atmosphere Flagship, Aspendale, Austalia, 27, 2014.

Gerbig, C., Lin, J. C., Wofsy, S. C., Daube, B. C., Andrews, A. E., Stephens, B. B., Bakwin, P. S., and Grainger, C. A.: Toward constraining regional-scale fluxes of CO_2 with atmospheric observations over a continent: 2. Analysis of COBRA data using a receptor-oriented framework, Journal of Geophysical Research: Atmospheres, 108, https://doi.org/10.1029/2003JD003770, 2003.

Gloor, M., Dlugokencky, E., Brenninkmeijer, C., Horowitz, L., Hurst, D. F., Dutton, G., Crevoisier, C., Machida, T., and Tans, P.: Three-dimensional SF_6 data and tropospheric transport simulations: Signals, modeling accuracy, and implications for inverse modeling, Journal of Geophysical Research: Atmospheres, 112, https://doi.org/10.1029/2006JD007973, 2007.

Gulev, S. K., Thorne, P. W., Ahn, J., Dentener, F. J., Domingues, C. M., Gerland, S., Gong, D., Kaufman, D. S., Nnamchi, H. C., Quaas, J., Rivera, J. A., Sathyendranath, S., Smith, S. L., Trewin, B., vo Shuckmann, K., and Vose, R. S.: Changing State of the Climate System, in:

Climate Change 2021: The Physical Science Basis. Contribution of Working Group I to the Sixth Assessment Report of the Intergovernmental Panel on Climate Change, edited by: Masson-Delmotte, V., Zhai, P., Pirani, A., Connors, S. L., Pean, C., Berger, S., Caud, N., Chen, Y., Goldfarb, L., Gomis, M. I., Huang, M., Leitzell, K., Lonnoy, E., Matthews, J. B. R., Maycock, T. K., Waterfield, T., Yelekci, O., Yu, P., and Zhou, B., Cambridge University Press, 2021.

Harnisch, J., Borchers, R., Fabian, P., and Maiss, M.: Tropospheric trends for CF_4 and C_2F_6 since 1982 derived from SF6 dated stratospheric air, Geophysical Research Letters, 23, 1099-1102, https://doi.org/10.1029/96GL01198, 1996.

Henne, S., Brunner, D., Oney, B., Leuenberger, M., Eugster, W., Bamberger, I., Meinhardt, F., Steinbacher, M., and Emmenegger, L.: Validation of the Swiss methane emission inventory by atmospheric observations and inverse modelling, Atmos. Chem. Phys., 16, 3683-3710, 10.5194/acp-16-3683-2016, 2016.

Hu, L., Montzka, S. A., Kaushik, A., Andrews, A. E., Sweeney, C., Miller, J., Baker, I. T., Denning, S., Campbell, E., Shiga, Y. P., Tans, P., Siso, M. C., Crotwell, M., McKain, K., Thoning, K., Hall, B., Vimont, I., Elkins, J. W., Whelan, M. E., and Suntharalingam, P.: COS-derived GPP relationships with temperature and light help explain high-latitude atmospheric CO_2 seasonal cycle amplification, Proceedings of the National Academy of Sciences, 118, e2103423118, 10.1073/pnas.2103423118, 2021.

Hu, L., Montzka, S. A., Lehman, S. J., Godwin, D. S., Miller, B. R., Andrews, A. E., Thoning, K., Miller, J. B., Sweeney, C., Siso, C., Elkins, J. W., Hall, B. D., Mondeel, D. J., Nance, D., Nehrkorn, T., Mountain, M., Fischer, M. L., Biraud, S. C., Chen, H., and Tans, P. P.: Considerable contribution of the Montreal Protocol to declining greenhouse gas emissions from the United States, Geophysical Research Letters, 44, 2017GL074388, 10.1002/2017GL074388, 2017.

Hu, L., Montzka, S. A., Miller, B. R., Andrews, A. E., Miller, J. B., Lehman, S. J., Sweeney, C., Miller, S. M., Thoning, K., Siso, C., Atlas, E. L., Blake, D. R., de Gouw, J., Gilman, J. B., Dutton, G., Elkins, J. W., Hall, B., Chen, H., Fischer, M. L., Mountain, M. E., Nehrkorn, T., Biraud, S. C., Moore, F. L., and Tans, P.: Continued emissions of carbon tetrachloride from the United States nearly two decades after its phaseout for dispersive uses, Proceedings of the National Academy of Sciences, 113, 2880-2885, 10.1073/pnas.1522284113, 2016.

Hu, L., Montzka, S. A., Miller, J. B., Andrews, A. E., Lehman, S. J., Miller, B. R., Thoning, K., Sweeney, C., Chen, H., Godwin, D. S., Masarie, K., Bruhwiler, L., Fischer, M. L., Biraud, S. C., Torn, M. S., Mountain, M., Nehrkorn, T., Eluszkiewicz, J., Miller, S., Draxler, R. R., Stein, A. F., Hall, B. D., Elkins, J. W., and Tans, P. P.: U.S. emissions of HFC-134a derived for 2008–2012 from an extensive flask-air sampling network, Journal of Geophysical Research: Atmospheres, 2014JD022617, 10.1002/2014JD022617, 2015.

Janssens-Maenhout, G.: EDGARv4.2 Emission Maps [dataset], 2011.

Levin, I., Naegler, T., Heinz, R., Osusko, D., Cuevas, E., Engel, A., Ilmberger, J., Langenfelds, R. L., Neininger, B., Rohden, C. v., Steele, L. P., Weller, R., Worthy, D. E., and Zimov, S. A.: The global SF_6 source inferred from long-term high precision atmospheric measurements and its comparison with emission inventories, Atmos. Chem. Phys., 10, 2655-2662, 10.5194/acp-10-2655-2010, 2010.

Lin, J. C., Gerbig, C., Wofsy, S. C., Andrews, A. E., Daube, B. C., Davis, K. J., and Grainger, C. A.: A near-field tool for simulating the upstream influence of atmospheric observations:

The Stochastic Time-Inverted Lagrangian Transport (STILT) model, Journal of Geophysical Research: Atmospheres, 108, 4493, 10.1029/2002jd003161, 2003.

Maiss, M. and Levin, I.: Global increase of SF_6 observed in the atmosphere, Geophysical Research Letters, 21, 569-572, https://doi.org/10.1029/94GL00179, 1994.

Maksyutov, S., Eggleston, S., HHun Woo, J., Fang, S., Witi, J., Gillenwater, M., Goodwin, J., and Tubiello, F.: Chapter 6: Quality Assurance / Quanlity Control and Verification, Intergovernmental Panel on Climate Change (IPCC), Kyoto, Japan, 2019.

Manning, A. J., Redington, A. L., Say, D., O'Doherty, S., Young, D., Simmonds, P. G., Vollmer, M. K., Mühle, J., Arduini, J., Spain, G., Wisher, A., Maione, M., Schuck, T. J., Stanley, K., Reimann, S., Engel, A., Krummel, P. B., Fraser, P. J., Harth, C. M., Salameh, P. K., Weiss, R. F., Gluckman, R., Brown, P. N., Watterson, J. D., and Arnold, T.: Evidence of a recent decline in UK emissions of hydrofluorocarbons determined by the InTEM inverse model and atmospheric measurements, Atmos. Chem. Phys., 21, 12739-12755, 10.5194/acp-21-12739-2021, 2021.

Michalak, A. M., Hirsch, A., Bruhwiler, L., Gurney, K. R., Peters, W., and Tans, P. P.: Maximum likelihood estimation of covariance parameters for Bayesian atmospheric trace gas surface flux inversions, Journal of Geophysical Research: Atmospheres, 110, D24107, 10.1029/2005jd005970, 2005.

Miller, S. M., Kort, E. A., Hirsch, A. I., Dlugokencky, E. J., Andrews, A. E., Xu, X., Tian, H., Nehrkorn, T., Eluszkiewicz, J., Michalak, A. M., and Wofsy, S. C.: Regional sources of nitrous oxide over the United States: Seasonal variation and spatial distribution, Journal of Geophysical Research: Atmospheres, 117, https://doi.org/10.1029/2011JD016951, 2012.

Miller, S. M., Wofsy, S. C., Michalak, A. M., Kort, E. A., Andrews, A. E., Biraud, S. C., Dlugokencky, E. J., Eluszkiewicz, J., Fischer, M. L., Janssens-Maenhout, G., Miller, B. R., Miller, J. B., Montzka, S. A., Nehrkorn, T., and Sweeney, C.: Anthropogenic emissions of methane in the United States, Proceedings of the National Academy of Sciences, 10.1073/pnas.1314392110, 2013.

Nehrkorn, T., Eluszkiewicz, J., Wofsy, S., Lin, J., Gerbig, C., Longo, M., and Freitas, S.: Coupled weather research and forecasting–stochastic time-inverted lagrangian transport (WRF–STILT) model, Meteorology and Atmospheric Physics, 107, 51-64, 10.1007/s00703-010-0068-x, 2010.

Nevison, C., Andrews, A., Thoning, K., Dlugokencky, E., Sweeney, C., Miller, S., Saikawa, E., Benmergui, J., Fischer, M., Mountain, M., and Nehrkorn, T.: Nitrous Oxide Emissions Estimated With the CarbonTracker-Lagrange North American Regional Inversion Framework, Global Biogeochemical Cycles, 32, 463-485, doi:10.1002/2017GB005759, 2018.

Orbe, C., Waugh, D. W., Montzka, S., Dlugokencky, E. J., Strahan, S., Steenrod, S. D., Strode, S., Elkins, J. W., Hall, B., Sweeney, C., Hintsa, E. J., Moore, F. L., and Penafiel, E.: Tropospheric Age-of-Air: Influence of SF6 Emissions on Recent Surface Trends and Model Biases, Journal of Geophysical Research: Atmospheres, 126, e2021JD035451, https://doi.org/10.1029/2021JD035451, 2021.

Ottinger, D., Averyt, M., and Harris, D.: US consumption and supplies of sulphur hexafluoride reported under the greenhouse gas reporting program, Journal of Integrative Environmental Sciences, 12, 5-16, 10.1080/1943815X.2015.1092452, 2015.

Peters, W., Krol, M. C., Dlugokencky, E. J., Dentener, F. J., Bergamaschi, P., Dutton, G., Velthoven, P. v., Miller, J. B., Bruhwiler, L., and Tans, P. P.: Toward regional-scale

642 modeling using the two-way nested global model TM5: Characterization of transport using
643 SF_6, Journal of Geophysical Research: Atmospheres, 109, D19314, 10.1029/2004jd005020,
644 2004.
645 Rand, S.: EPA's SF6 Emission Reduction Partnership for Electric Power Systems, 2012.
646 Ray, E. A., Moore, F. L., Elkins, J. W., Rosenlof, K. H., Laube, J. C., Röckmann, T., Marsh, D.
647 R., and Andrews, A. E.: Quantification of the SF_6 lifetime based on mesospheric loss
648 measured in the stratospheric polar vortex, Journal of Geophysical Research: Atmospheres,
649 122, 4626-4638, https://doi.org/10.1002/2016JD026198, 2017.
650 Rigby, M., Mühle, J., Miller, B. R., Prinn, R. G., Krummel, P. B., Steele, L. P., Fraser, P. J.,
651 Salameh, P. K., Harth, C. M., Weiss, R. F., Greally, B. R., O'Doherty, S., Simmonds, P.
652 G., Vollmer, M. K., Reimann, S., Kim, J., Kim, K. R., Wang, H. J., Olivier, J. G. J.,
653 Dlugokencky, E. J., Dutton, G. S., Hall, B. D., and Elkins, J. W.: History of atmospheric
654 SF_6 from 1973 to 2008, Atmos. Chem. Phys., 10, 10305-10320, 10.5194/acp-10-10305-
655 2010, 2010.
656 Rodgers, C. D.: Inverse Methods for Atmospheric Sounding, World Sci., Oxford, 10.1142/3171,
657 2000.
658 Schuh, A. E., Jacobson, A. R., Basu, S., Weir, B., Baker, D., Bowman, K., Chevallier, F., Crowell,
659 S., Davis, K. J., Deng, F., Denning, S., Feng, L., Jones, D., Liu, J., and Palmer, P. I.:
660 Quantifying the Impact of Atmospheric Transport Uncertainty on CO_2 Surface Flux
661 Estimates, Global Biogeochemical Cycles, 33, 484-500,
662 https://doi.org/10.1029/2018GB006086, 2019.
663 Simmonds, P. G., Rigby, M., Manning, A. J., Park, S., Stanley, K. M., McCulloch, A., Henne, S.,
664 Graziosi, F., Maione, M., Arduini, J., Reimann, S., Vollmer, M. K., Mühle, J., O'Doherty,
665 S., Young, D., Krummel, P. B., Fraser, P. J., Weiss, R. F., Salameh, P. K., Harth, C. M.,
666 Park, M. K., Park, H., Arnold, T., Rennick, C., Steele, L. P., Mitrevski, B., Wang, R. H. J.,
667 and Prinn, R. G.: The increasing atmospheric burden of the greenhouse gas sulfur
668 hexafluoride (SF_6), Atmos. Chem. Phys., 20, 7271-7290, 10.5194/acp-20-7271-2020, 2020.
669 Stein, A. F., Draxler, R. R., Rolph, G. D., Stunder, B. J. B., Cohen, M. D., and Ngan, F.: NOAA's
670 HYSPLIT atmospheric transport and dispersion modeling system, Bulletin of the
671 American Meteorological Society, 10.1175/BAMS-D-14-00110.1, 2015.
672 U.S. Energy Information Administration: Hourly electricity consumption varies throughout the
673 day and across seasons:
674 https://www.eia.gov/todayinenergy/detail.php?id=42915#:~:text=During%20the%20wint
675 er%20months%2C%20hourly,for%20space%20heating%20or%20cooling, last access: Jul
676 7, 2020.
677 U.S. Environmental Protection Agency: Inventory of U.S. Greenhouse Gas Emissions and Sinks:
678 1990-2020EPA 430-R-22-003, 2022a.
679 U.S. Environmental Protection Agency: Inventory of U.S. Greenhouse Gas Emissions and Sinks
680 by State: https://www.epa.gov/ghgemissions/state-ghg-emissions-and-removals, 2022b.
681 U.S. Federal Emergency Management Agency: United States transmission grid, 2008, publised on
682 https://en.wikipedia.org/wiki/North_American_power_transmission_grid#/media/File:Un
683 itedStatesPowerGrid.jpg, last access: Apr 5, 2022.
684 Waugh, D. W., Crotwell, A. M., Dlugokencky, E. J., Dutton, G. S., Elkins, J. W., Hall, B. D.,
685 Hintsa, E. J., Hurst, D. F., Montzka, S. A., Mondeel, D. J., Moore, F. L., Nance, J. D., Ray,
686 E. A., Steenrod, S. D., Strahan, S. E., and Sweeney, C.: Tropospheric SF_6: Age of air from

the Northern Hemisphere midlatitude surface, Journal of Geophysical Research: Atmospheres, 118, 11,429-411,441, https://doi.org/10.1002/jgrd.50848, 2013.

Weiss, R. F. and Prinn, R. G.: Quantifying greenhouse-gas emissions from atmospheric measurements: a critical reality check for climate legislation, Philosophical Transactions of the Royal Society A: Mathematical, Physical and Engineering Sciences, 369, 1925-1942, doi:10.1098/rsta.2011.0006, 2011.

Table 1. U.S. national and regional annual emissions of SF_6 (in Gg yr^{-1}) reported by EPA and derived from NOAA atmospheric measurements from this study. Errors derived from NOAA atmospheric measurements are expressed at a 95% confidence interval.

Year	National totals		Regions											
			Northeast		Southeast		Central North		Central South		Mountain		West	
	EPA	NOAA	EPA	NOAA	EPA	NOAA	EPA	NOAA	EPA	NOAA	EPA	NOAA	EPA	NOAA
2007	0.40	0.83±0.19	0.04	0.18±0.10	0.03	0.05±0.07	0.16	0.30±0.07	0.06	0.22±0.07	0.07	0.04±0.03	0.04	0.03±0.07
2008	0.37	1.03±0.26	0.05	0.22±0.10	0.02	0.09±0.07	0.13	0.34±0.14	0.06	0.28±0.09	0.06	0.06±0.04	0.03	0.04±0.06
2009	0.32	0.75±0.26	0.04	0.16±0.10	0.03	0.08±0.05	0.10	0.25±0.13	0.06	0.22±0.10	0.06	0.02±0.03	0.03	0.02±0.04
2010	0.32	0.63±0.16	0.04	0.12±0.04	0.02	0.05±0.03	0.11	0.20±0.08	0.06	0.12±0.04	0.06	0.05±0.02	0.03	0.08±0.04
2011	0.36	0.58±0.12	0.04	0.13±0.04	0.03	0.06±0.02	0.14	0.19±0.05	0.06	0.11±0.03	0.06	0.03±0.02	0.03	0.06±0.02
2012	0.30	0.40±0.11	0.04	0.09±0.05	0.03	0.04±0.03	0.10	0.13±0.03	0.05	0.08±0.03	0.05	0.03±0.02	0.03	0.04±0.02
2013	0.28	0.40±0.12	0.04	0.11±0.07	0.03	0.03±0.03	0.08	0.13±0.04	0.04	0.08±0.03	0.05	0.02±0.02	0.03	0.03±0.02
2014	0.29	0.48±0.14	0.04	0.15±0.09	0.03	0.05±0.03	0.09	0.13±0.04	0.05	0.08±0.03	0.05	0.03±0.02	0.03	0.03±0.02
2015	0.24	0.43±0.14	0.04	0.13±0.05	0.02	0.05±0.03	0.08	0.13±0.04	0.04	0.07±0.02	0.04	0.03±0.02	0.02	0.03±0.02
2016	0.26	0.40±0.09	0.04	0.12±0.04	0.03	0.04±0.02	0.10	0.11±0.03	0.04	0.08±0.04	0.04	0.02±0.02	0.02	0.02±0.02
2017	0.26	0.35±0.12	0.03	0.09±0.04	0.03	0.03±0.03	0.09	0.10±0.03	0.04	0.08±0.04	0.04	0.03±0.03	0.02	0.02±0.02
2018	0.25	0.39±0.12	0.03	0.09±0.02	0.03	0.07±0.04	0.09	0.11±0.03	0.04	0.08±0.04	0.04	0.02±0.02	0.02	0.03±0.03

Figures

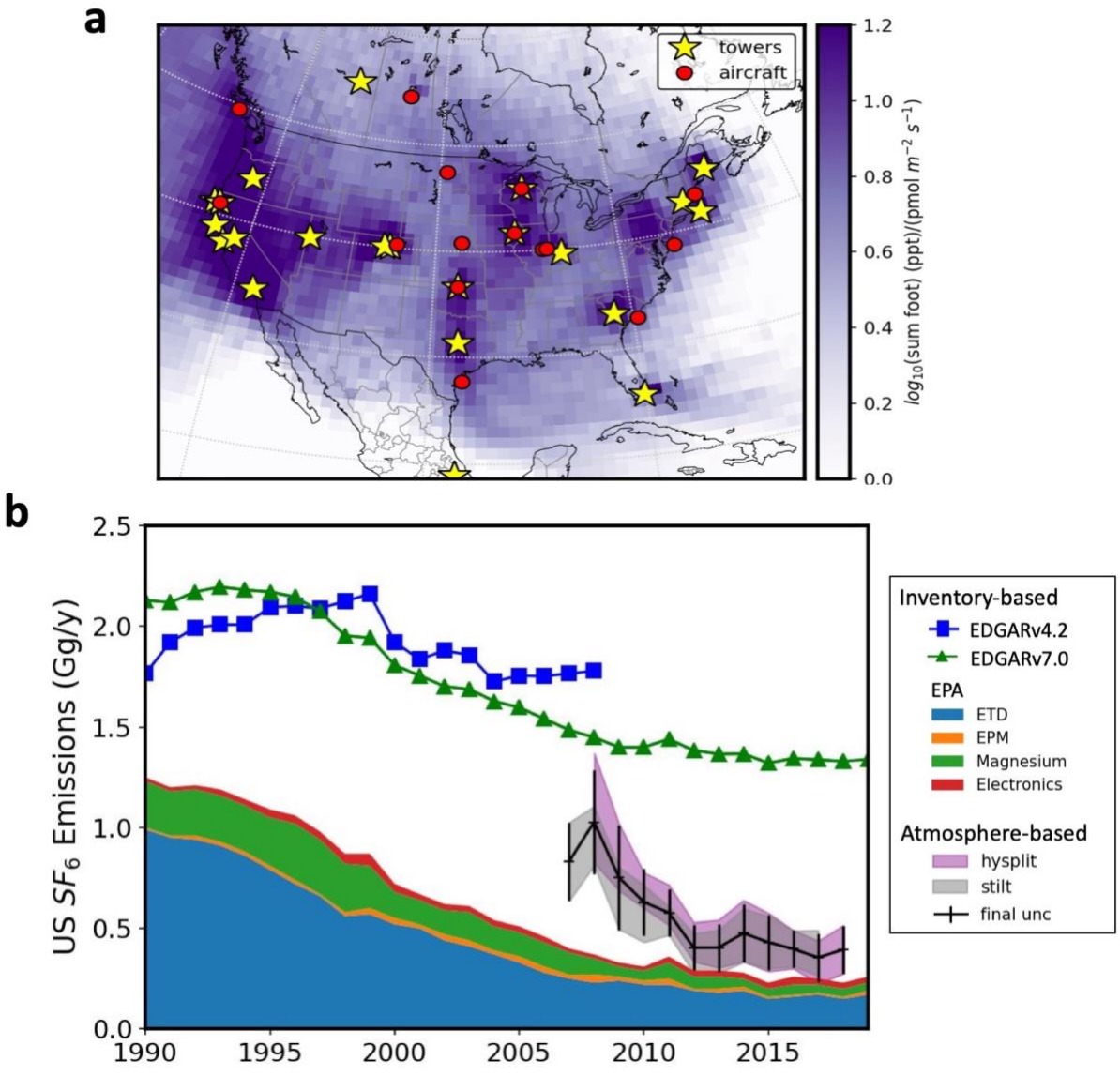

Fig. 1. U.S. SF_6 emissions derived from atmospheric observations and reported by inventories. (a) Locations of atmospheric SF_6 measurements considered in the regional inversions; tower-based sampling is indicated as stars and airborne-profile sampling is denoted as circles. Sensitivity of the atmospheric SF_6 measurements to surface emissions is indicated on a log10 scale as purple shading. (b) U.S. SF_6 emissions reported by EDGAR (v4.2 and v7.0) and EPA inventories, and derived from atmospheric observations. National totals are shown from EDGARv7.0, whereas the EPA inventory is parsed out by sector, including electric power transmission and distribution (ETD), electrical equipment manufacturing (EPM), magnesium production, and electronics. Atmosphere-based emission estimates for the contiguous U.S. are derived with two different model analyses of the atmospheric observations using two different transport simulations (HYSPLIT-NAMS in purple shading for 2008 - 2018 and WRF-STILT in gray shading for 2007 - 2017). The black line with error bars indicates inversion ensemble annual means and an uncertainty at a 95% confidence interval.

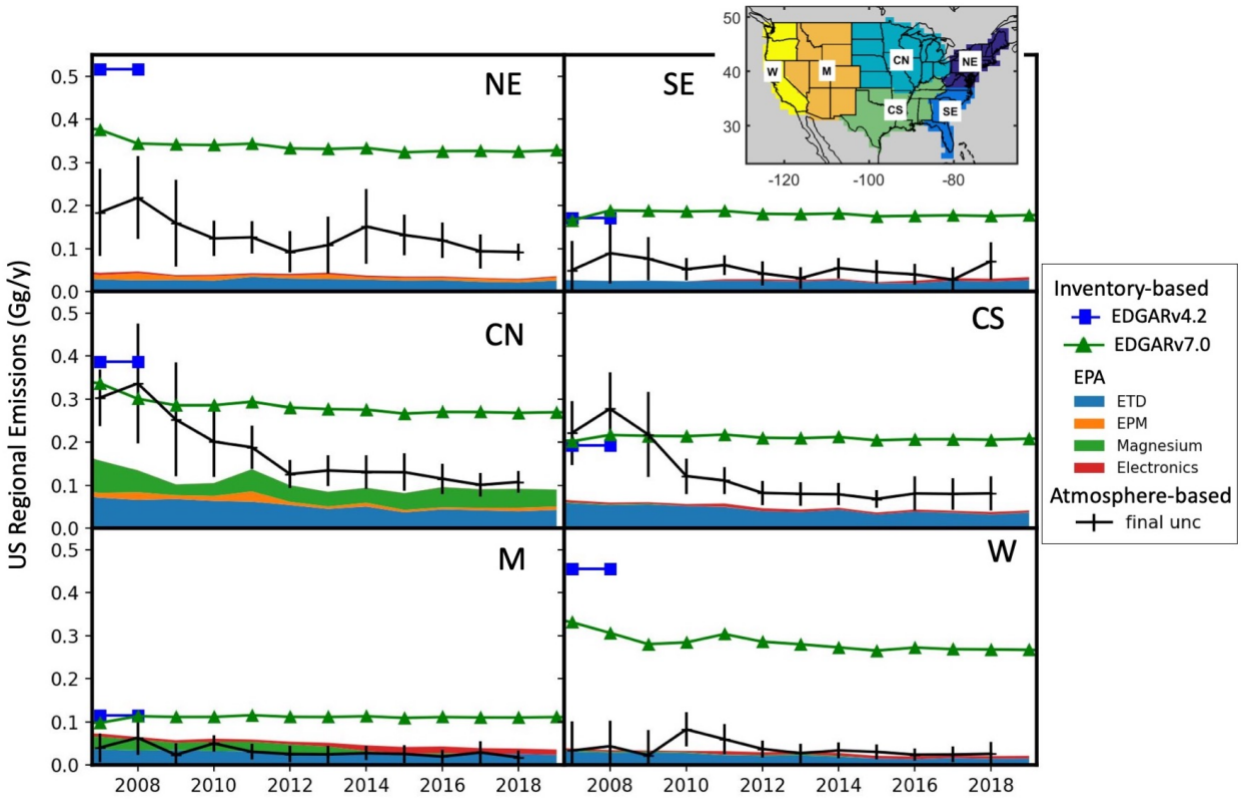

Fig. 2. Regional SF_6 emissions over the U.S., derived from atmospheric observations and reported by EPA's GHGI and EDGAR (EDGARv4.2 and EDGARv7.0). EPA emissions are parsed out by sectors, i.e., electrical transformation and distribution (ETD), electrical power manufacturing (EPM), magnesium production, and electronics, while EDGAR emissions are presented as totals. Atmosphere-based emission estimates (black lines) include uncertainties at a 95% confidence interval (vertical black bars).

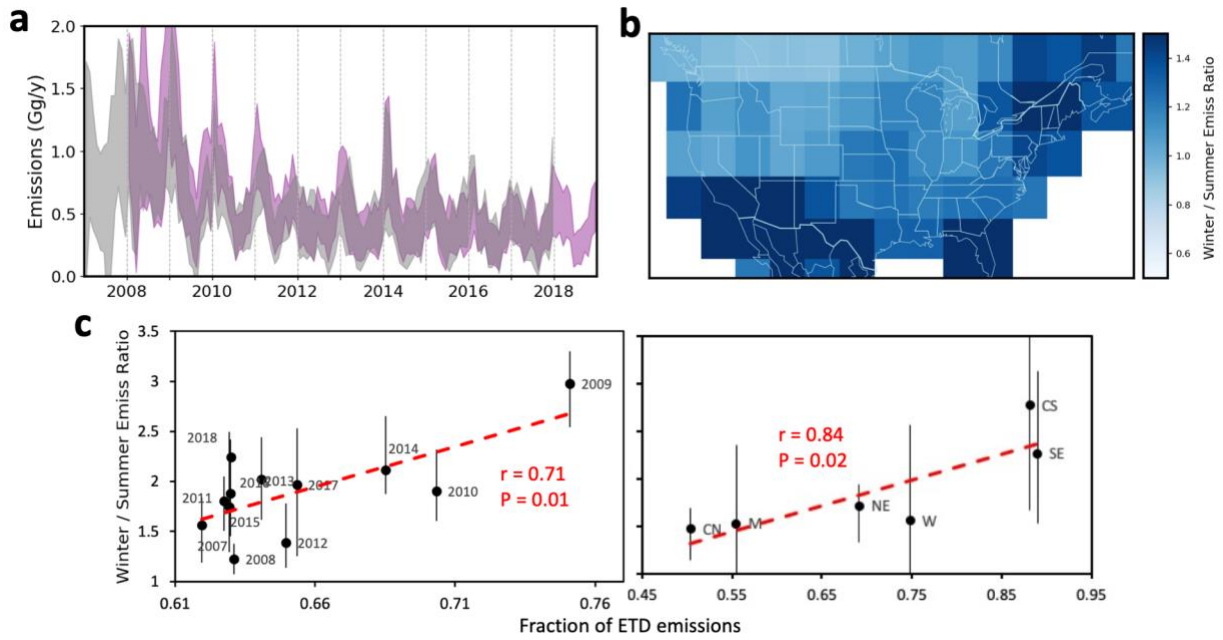

Fig. 3. Seasonal cycle of U.S. SF_6 emissions derived from atmospheric observations. (a) Monthly emissions derived from atmospheric inversions using HYSPLIT-NAMS (in purple shading) and WRF-STILT (in gray shading) transport simulations. The shading associated with each transport model represents a combined uncertainty associated with 6 different inversions. (b) The winter-to-summer emission ratios derived on a $5^o \times 5^o$ grid from atmospheric observations, averaged across all years and 12 inversion ensemble members. The winter and summer here are defined as Nov – Feb and May – Aug. (c) Atmosphere-derived winter-to-summer emission ratios versus the fraction of total U.S. SF_6 emissions from electric power transformation and distribution (ETD) reported by EPA. Left: the ETD emission fraction versus winter-to-summer emission ratios for annual national emissions; errorbars indicate the 2.5^{th} – 97.5^{th} percentile range from the 12 inversion ensembles. Right: the mean ETD emission fraction by region averaged between 2007-2018 versus winter-to-summer emission ratios for multi-year average regional emissions over the same period; errorbars indicate the 2.5^{th} – 97.5^{th} percentile range from the 12 inversion ensembles.